

Disorder-induced reversal of spin polarization in the Heusler alloy Co_2FeSi

P. Bruski,^{1,*} S. C. Erwin,² M. Ramsteiner,¹ O. Brandt,¹ K.-J. Friedland,¹ R. Farshchi,¹ J. Herfort,¹ and H. Riechert¹

¹*Paul-Drude Institut für Festkörperelektronik, Hausvogteiplatz 5–7, D-10117 Berlin, Germany*

²*Center for Computational Materials Science, Naval Research Laboratory, Washington, DC 20375, USA*

(Received 3 March 2011; published 25 April 2011)

We study the spin polarization in the conduction band of Co_2FeSi layers with a different degree of structural order. The injected spin polarization in $\text{Co}_2\text{FeSi}/(\text{Al,Ga})\text{As}$ spin light-emitting diodes as well as the planar Hall effect measured for the Co_2FeSi injectors exhibit a sign reversal between injectors crystallized in the ordered $L2_1$ phase and the Fe-Si disordered $B2$ phase. These results are explained by a disorder-induced change in the spin polarization at the Fermi energy of Co_2FeSi . Support for the occurrence of such a striking change in the electronic band structure is obtained by first principles calculations.

DOI: [10.1103/PhysRevB.83.140409](https://doi.org/10.1103/PhysRevB.83.140409)

PACS number(s): 75.50.Bb, 72.25.Dc, 72.25.Mk, 81.15.Hi

In the field of spintronics, electrical spin injection from ferromagnetic metals has become an important building block for potential device applications.^{1–5} Half metals are ideal spin injectors because of their 100% spin polarization at the Fermi energy. The Heusler alloy Co_2FeSi is predicted to be a half metal in its ordered $L2_1$ phase⁶ and has the additional advantage of being closely lattice matched to GaAs, allowing for the synthesis of high-quality epitaxial layers on $(\text{Al,Ga})\text{As}/\text{GaAs}$ heterostructures.^{7,8} In fact, Co_2FeSi in its $L2_1$ phase grown by molecular-beam epitaxy (MBE) has already been demonstrated to be a very promising material for spin injection into $(\text{Al,Ga})\text{As}/\text{GaAs}$ spin light-emitting diodes (LEDs) with a spin-injection efficiency of more than 50%.⁹

The $L2_1$ phase is obtained by MBE growth at a substrate temperature (T_S) around 300 °C, while for lower T_S , it is found to coexist with the $B2$ phase which is defined by a complete disorder in the Fe-Si sublattice only. This partially disordered phase even dominates at low T_S , at least in a region close to the $(\text{Al,Ga})\text{As}$ interface.¹⁰ However, the hybrid system $\text{Co}_2\text{FeSi}/(\text{Al,Ga})\text{As}$ suffers from massive diffusion of Co and Fe into $(\text{Al,Ga})\text{As}$ during growth at elevated temperature.^{9,11} This undesirable process is thermally activated and can at least be partially suppressed by using low growth temperatures which, however, result in Co_2FeSi layers exhibiting a relatively large volume fraction of the $B2$ phase.¹⁰

Analogously to other Heusler alloys,^{12,13} it is likely that Co_2FeSi is not half metallic in the $B2$ phase, which thus would lower the maximum achievable spin-injection efficiency. For elucidating the suspected differences in the spin-dependent electronic band structure between the $L2_1$ and $B2$ phases, we investigate the degree of circular polarization of the electroluminescence (EL) of a series of spin LEDs with Co_2FeSi injection layers grown by MBE at different T_S . These experiments are complemented by planar Hall-effect measurements and first-principles band-structure calculations based on the density-functional theory (DFT) including the Coulomb parameter U (DFT+ U). Our results demonstrate that the spin polarization of Co_2FeSi at the Fermi edge reverses its sign with the introduction of $B2$ disorder.

The spin LEDs were grown in a dual-chamber MBE with the semiconductor structure containing a $\text{GaAs}/(\text{Al,Ga})\text{As}$ quantum well. Details of their design and growth are given in Refs. 9 and 11. The individual spin-LED structures of the investigated sample series differ only by the substrate

temperature T_S used for the MBE growth of the Co_2FeSi injector layer. For the lowest growth temperature, the substrate was not intentionally heated, but was nonetheless heated by the radiation of the hot Co, Fe, and Si effusion cells. The actual growth temperature is estimated to be about 20 to 60 °C. LED #B2 was thermally annealed at 300 °C to improve its EL intensity. This post-growth annealing effectively removes nonradiative defects at the $\text{Co}_2\text{FeSi}/(\text{Al,Ga})\text{As}$ interface,⁹ but does not affect the long-range ordering ($B2$ vs $L2_1$ phase) as well as the magnetic properties of the Co_2FeSi layer and has a negligible effect on the interdiffusion at the $(\text{Al,Ga})\text{As}$ interface.¹⁴ The electroluminescence (EL) measurements were performed at 20 K in Faraday geometry with the LEDs placed in a superconducting magnet system.^{9,11} As a measure of the spin-injection efficiency, we analyzed the degree of circular polarization P_{EL} . Anisotropic magneto-resistance (AMR) experiments were performed on rectangular samples with Ohmic contacts applied such that a homogeneous current could be driven along the $[\bar{1}10]$ hard axis or the $[110]$ easy axis of magnetization. We will focus here on the transversal magneto-resistance ρ_{xy} , which is referred to as the planar Hall effect and which was measured as a function of the angle θ_B between the external in-plane magnetic field and the current direction.^{15–17} An external in-plane magnetic field of $B = 0.4$ T (i.e., sufficient to reach the saturation magnetization) was applied, where $\theta_M = \theta_B$ with θ_M being the angle of magnetization with respect to the direction of the electrical current.^{15–17} The experiments were carried out at a sample temperature of 295 K and a current of 1 mA. The Curie temperature of Co_2FeSi is about 1100 K for the $L2_1$ phase¹⁸ and can be estimated to be above 890 K for the $B2$ phase¹⁹ (i.e., well above all sample temperatures in the measurements described here).

The electronic density of states (DOS) was calculated for the $L2_1$ and $B2$ bulk phases within density-functional theory (DFT) in the PBE generalized-gradient approximation (GGA), using projector-augmented-wave potentials as implemented in VASP.^{20,21} To properly account for onsite electronic correlation in the Co and Fe $3d$ states we adopted the DFT+ U approach, using effective U parameters ($U_{\text{Co}} = 1.9$, $U_{\text{Fe}} = 1.8$ eV) from Fecher and Felser in their treatment of the $\text{CoFeAl}_{1-x}\text{Si}_x$ Heusler alloy series.²² Please note that the Gilbert damping constant cannot be used as the preferred parameter to evaluate the accuracy of the underlying electronic structure calculation

since even very accurate first-principles calculations do not result in a satisfactory agreement with experimental values.²³ For the ordered $L2_1$ phase, our pseudopotential plane-wave results for band structure and density of states are indistinguishable from their full-potential results. For the disordered $B2$ phase we represented the Fe-Si site disorder using appropriately defined “special quasirandom structures” (SQS), which were originally developed for treating site disorder in compound semiconductor alloys.²⁴ We tested two SQS supercells, each containing four Co_2FeSi formula units, based on two different criteria for approximating the local correlations of the perfectly random phase.²⁵ The resulting DOS for these two SQS supercells were very similar and so below we discuss the results for just one, reasonably confident that it accurately reflects the electronic structure of the truly random disordered phase.

Figure 1 displays P_{EL} of LED #B2 and LED #L2 as a function of the external magnetic field. The P_{EL} curves of both spin LEDs clearly demonstrate the presence of spin injection from Co_2FeSi since they track exactly the out-of-plane magnetization of the injector material determined by superconducting quantum interference device (SQUID) magnetometry. The absolute values of the polarization in the saturation range for LED #B2 (9%) and LED #L2 (18%) correspond to spin-injection efficiencies of at least 27% and 54%, respectively.^{9,11} However, the most striking difference between LED #B2 and LED #L2 is the opposite sign of P_{EL} . The sign of P_{EL} reflects the spin polarization of electrons reaching the active region of the spin LED after being injected from Co_2FeSi into the top (Al,Ga)As layer. This spin polarization is directly related to the electronic band structure of the respective injector layers (i.e., a sign reversal of P_{EL} reflects an opposite majority-spin orientation at the Fermi energy in the conduction band of the two different Co_2FeSi layers in LED #B2 and LED #L2). Due to their different growth temperatures, the Co_2FeSi layer of LED #L2 is expected to consist entirely of the $L2_1$ phase, whereas a substantial

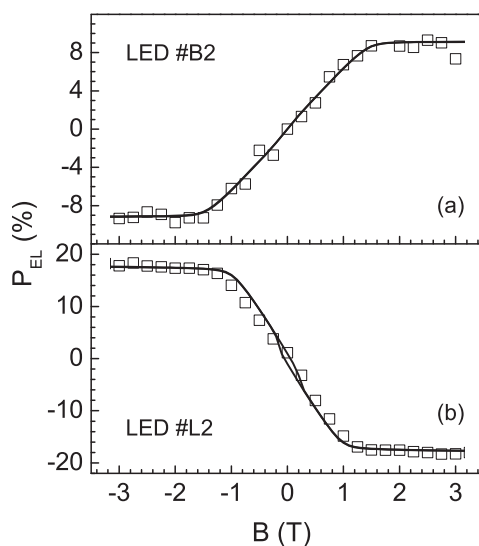


FIG. 1. Degree of circular polarization of the EL signal (P_{EL} as symbols) as a function of the external magnetic field B from (a) LED #B2 and (b) LED #L2 together with the Co_2FeSi out-of-plane magnetization curve (solid line in arbitrary units).

volume fraction of the Fe-Si disordered $B2$ phase is certain to exist in the Co_2FeSi layer of LED #B2.¹⁰ We thus interpret our experimental finding such that the injection process is dominated by the $B2$ phase in LED #B2 and the $L2_1$ phase in LED #L2 with the two different Co_2FeSi phases exhibiting *opposite spin polarizations* at the Fermi energy.

Our finding of opposite spin polarization in the two different Co_2FeSi phases has an important consequence for injector layers consisting of a spatially inhomogeneous distribution of the $L2_1$ and $B2$ phases. As it is evident from studies using transmission electron microscopy, both phases are present close to the semiconductor interface for $150^\circ\text{C} < T_S < 250^\circ\text{C}$ as shown, for example, in Ref. 10. Consequently, the total spin-injection efficiency for such injector layers includes contributions from both phases, which should thus partially compensate each other.

In order to verify this idea, we record P_{EL} for a whole set of samples grown at $T_S < 320^\circ\text{C}$. Note that for this sample series the diffusion of Co and Fe during growth into the topmost (Al,Ga)As of the spin LEDs was considerably reduced as compared to the samples investigated in our previous work (Refs. 9 and 11) owing to slight changes in the growth parameters. These improvements allow us to detect spin injection with the ferromagnetic Co_2FeSi signature by EL measurements for all samples. Figure 2 displays P_{EL} in the saturation range ($|B| > 1.5$ T) as a function of T_S . Indeed, as expected from our model of coexisting $L2_1$ and $B2$ phases with opposite spin polarizations at the Fermi energy, only relatively small values of P_{EL} are obtained for $140^\circ\text{C} < T_S < 280^\circ\text{C}$ (regime II). The large values of P_{EL} observed for LED #B2 and LED #L2 arise from interface regions that are predominantly $B2$ and $L2_1$, respectively. Growth temperatures higher than 280°C (regime III) lead to a reduction of the EL polarization degree due to interfacial reactions²⁶ and the fact that the diffusion of Co and Fe leads to a degradation of the quantum well in the active region of the LEDs. The diffusion of Co and Fe into (Al,Ga)As:Si has been found to depend very sensitively on the Al content as well as the Si doping density. Therefore, slight changes in

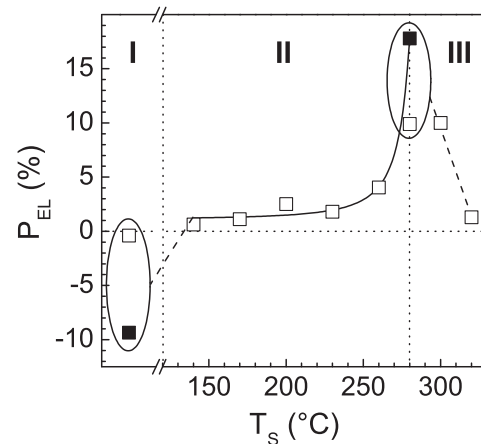


FIG. 2. Degree of circular polarization of the EL signal (P_{EL} at $|B| > 1.5$ T) as a function of T_S of the Co_2FeSi film. In regime I, the substrate was not heated during the Co_2FeSi growth. The solid symbols correspond to LED #B2 and LED #L2 (cf. Figs. 1 and 5). The lines are guides to the eye.

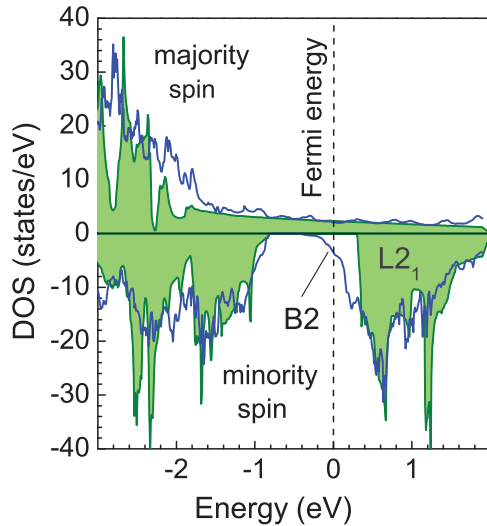


FIG. 3. (Color online) Calculated electronic density of states for the highly ordered $L2_1$ (shaded) and the disordered $B2$ (solid line) phase of Co_2FeSi , displayed separately for the majority-spin and minority-spin states.

these parameters as well as the growth temperature lead to considerable changes in the amount of Co and Fe diffusing into the topmost (Al,Ga)As:Si layer of the spin LEDs. Such diffusion processes into the semiconductor part of the spin LEDs influence strongly the detectability of the spin-injection process, particularly the EL polarization in the saturation range (see Fig. 2), but not the structural and electronic properties of the ferromagnetic injector layer.¹¹ The above statements hold in particular for samples grown without intentional heating of the substrate. As indicated in Fig. 2 by additional data points in regime I (no substrate heating) and for $T_S = 280^\circ\text{C}$, the small variations in the growth conditions lead to different values of P_{EL} , but the sign of P_{EL} remains unchanged.

The calculated electronic density of states (DOS) of Co_2FeSi is displayed in Fig. 3 for both the $B2$ and $L2_1$ phases. The DOS of the $L2_1$ phase exhibits the usual half-metallic gap for minority-spin electrons around the Fermi energy. For the $B2$ phase, in contrast, this gap is partially filled in. Indeed, at the Fermi energy the resulting density of states for minority spins is even larger than for majority spins. This result is qualitatively consistent with our experimental finding that $B2$ disorder leads to a reversal of the spin polarization.

Figure 4 illustrates this effect quantitatively, as a function of the Coulomb U parameter. For U less than about 2.2 eV, we obtain a negative spin polarization P_N based on the density of states (N). Figure 4 also shows the spin polarization P_{Nv_x} derived by Mazin to describe spin-polarized ballistic tunneling between a ferromagnet and a normal metal.²⁷ For spin injection from a ferromagnetic metal into a semiconductor an analogous derivation can be made, with the result that for each spin the number of conductance channels is proportional to the Fermi-surface average $\langle Nv_x \rangle$. For this definition the trend is similar: smaller values of U push the spin polarization toward a sign reversal. It is important to note, that for the tunneling case some controversy exists in the literature regarding the appropriate choice for the definition of spin polarization. In Refs. 28 and 29, for example, the bare density of states (P_N) is given as the

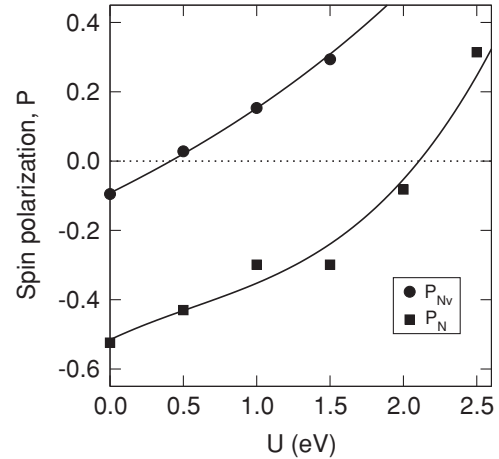


FIG. 4. Theoretical spin polarization P_N (squares) and P_{Nv} (circles) at the Fermi energy for the $B2$ phase of Co_2FeSi , as a function of the Coulomb parameter U .

correct choice. Since the ferromagnet/semiconductor interface is commonly regarded as a Schottky tunneling contact, our experimental findings are indeed supported by the DFT + U calculations for a reasonable range of the Coulomb U parameter.

A point which has to be considered is the following: Since the spin diffusion length in ferromagnetic metals is typically on the order of only a few nm,³⁰ the EL experiments described above are most sensitive to the ferromagnet/semiconductor interface region. Recently, Khosravizadeh *et al.* used density-functional theory to analyze the electronic structure of different $\text{Co}_2\text{FeSi}/\text{GaAs}$ interface terminations. For all the terminations studied the result was qualitatively the same: the interfacial atomic layer exhibits negative spin polarization, while all deeper layers are nearly bulklike.³¹ From their work it is evident that the $L2_1/\text{GaAs}$ and $B2/\text{GaAs}$ interfaces should be very similar electronically. Since the experiments show, on

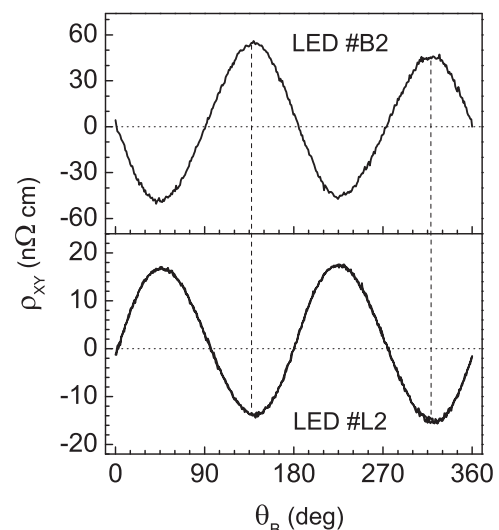


FIG. 5. Transverse resistivity ρ_{xy} (planar Hall effect) for LED #B2 and LED #L2 as a function of the angle $\theta_B = \theta_M$ at an external in-plane magnetic field of $B = 0.4$ T (saturated magnetization).

the contrary, opposite behavior it is evident that the interface plays no significant role.

Furthermore, we performed magneto-transport experiments with an in-plane external magnetic field which probe the properties of the entire Co_2FeSi layer and are less sensitive to the interface to the semiconductor as compared to the above EL experiments involving spin injection. In fact, we have found both the AMR as well as the amplitude of the planar Hall effect (transverse resistivity) to exhibit a clear dependence on T_S , the growth temperature of the Co_2FeSi layer. This finding suggests that the AMR and the planar Hall effect can both be utilized as a measure for the relative volume fractions of the $B2$ and $L2_1$ phases (which changes with T_S as explained above). Figure 5 displays the transverse resistivity ρ_{xy} (planar Hall effect) for the two limiting cases of LED #B2 and LED #L2 as a function of the angle $\theta_B = \theta_M$ ($B = 0.4$ T). The ρ_{xy} for the two samples is seen to be phase-shifted by $\pi/2$ in θ_B , equivalent to a sign reversal in the planar Hall effect. This result directly demonstrates that the sign reversal observed in spin injection is in fact related to the properties of the respective Co_2FeSi phase and not to an interface effect such as spin filtering.

According to the conventional phenomenological AMR theory for isotropic materials,^{31,32} the angle-dependent transverse resistance is given by $\rho_{xy} = \frac{1}{2}(\rho_{\parallel} - \rho_{\perp}) \sin(2\theta_M)$ with the longitudinal resistivities ρ_{\parallel} and ρ_{\perp} for the current parallel and perpendicular to the magnetization, respectively. Since $(\rho_{\parallel} - \rho_{\perp})$ has been measured to be negative for both LED #B2 and LED #L2, the above expression for ρ_{xy} is not able to account for our experimental observation of sign reversal which, therefore, cannot be explained in the framework of the conventional AMR theory for isotropic materials, similarly to

the effects observed in Fe and Fe_3Si .^{15,16} Since the same result is obtained for both current directions along $[\bar{1}10]$ (hard axis of magnetization) and $[110]$ (easy axis of magnetization), any anisotropy related to the crystal structure can be ruled out as origin for the sign reversal. Instead, our observation can be explained by the appearance of an additional spin-dependent anisotropy^{31,33} reflecting the opposite spin polarization at the Fermi energy of the $B2$ and $L2_1$ phases in strong support of our above conclusions concerning their electronic structures.³⁴ A detailed description of the magneto-transport results will be published elsewhere.

In conclusion, spin injection and planar-Hall effect experiments provide evidence for a disorder-induced sign reversal of the spin polarization in the conduction band of Co_2FeSi . This experimental finding is supported by first-principle calculations of the electronic density of states for both the ordered $L2_1$ and the disordered $B2$ phase. Our findings provide an important insight into the impact of disorder on the electronic characteristics of a Heusler alloy, which has been demonstrated to be a very promising spin-injector material.

We are grateful to Igor Mazin for enlightening discussions, to Alberto Hernández-Mínguez for critical manuscript reading, and to Walid Anders, Claudia Herrmann, Angela Riedel, and Gerd Paris for technical support. S.C.E. acknowledges support from the Office of Naval Research. Computations were performed at the DoD Major Shared Resource Center at Air Force Research Laboratory. R.F. acknowledges support from the Alexander von Humboldt Foundation.

*bruski@pdi-berlin.de

- ¹H. J. Zhu *et al.*, *Phys. Rev. Lett.* **87**, 016601 (2001).
- ²A. T. Hanbicki *et al.*, *Appl. Phys. Lett.* **80**, 1240 (2002).
- ³V. F. Motsnyi *et al.*, *Phys. Rev. B* **68**, 245319 (2003).
- ⁴C. Adelman *et al.*, *Phys. Rev. B* **71**, 121301 (2005).
- ⁵X. Jiang *et al.*, *Phys. Rev. Lett.* **94**, 056601 (2005).
- ⁶S. Wurmehl *et al.*, *Phys. Rev. B* **72**, 184434 (2005).
- ⁷M. Hashimoto *et al.*, *Appl. Phys. Lett.* **87**, 102506 (2005).
- ⁸M. Hashimoto *et al.*, *J. Cryst. Growth* **301**, 592 (2007).
- ⁹M. Ramsteiner *et al.*, *Phys. Rev. B* **78**, 121303(R) (2008).
- ¹⁰M. Hashimoto *et al.*, *J. Vac. Sci. Technol. B* **25**, 1453 (2007).
- ¹¹O. Brandt *et al.*, *Phys. Rev. B* **81**, 115302 (2010).
- ¹²H. C. Kandpal *et al.*, *Phys. Rev. B* **73**, 094422 (2006).
- ¹³G. H. Fecher *et al.*, *J. Phys. D: Appl. Phys.* **40**, 1576 (2007).
- ¹⁴K. Kumakura, H.-P. Schönherr, and J. Herfort (unpublished).
- ¹⁵M. Bowen *et al.*, *Phys. Rev. B* **71**, 172401 (2005).
- ¹⁶M. Bowen *et al.*, *Europhys. Lett.* **74**, 163 (2006).
- ¹⁷K.-J. Friedland *et al.*, *J. Phys. Condens. Matter* **18**, 2641 (2006).
- ¹⁸S. Wurmehl *et al.*, *Appl. Phys. Lett.* **88**, 032503 (2006).
- ¹⁹V. Niculescu *et al.*, *Phys. Rev. B* **19**, 452 (1979).
- ²⁰G. Kresse and J. Hafner, *Phys. Rev. B* **47**, 558 (1993).
- ²¹G. Kresse and J. Furthmüller, *Phys. Rev. B* **54**, 11169 (1996).
- ²²G. H. Fecher and C. Felser, *J. Phys. D: Appl. Phys.* **40**, 1582 (2007).
- ²³K. Gilmore *et al.*, *Phys. Rev. Lett.* **99**, 027204 (2007).
- ²⁴A. Zunger *et al.*, *Phys. Rev. Lett.* **65**, 353 (1990).
- ²⁵A. van de Walle *et al.*, *Calphad* **26**, 539 (2002).
- ²⁶M. Hashimoto *et al.*, *J. Phys. D: Appl. Phys.* **40**, 1631 (2007).
- ²⁷I. I. Mazin, *Phys. Rev. Lett.* **83**, 1427 (1999).
- ²⁸H. X. Tang *et al.*, in *Semiconductor Spintronics and Quantum Computation*, edited by D. D. Awschalom, D. Loss, and N. Samarth (Springer, Berlin, 2002).
- ²⁹S. Sanvito, in *Handbook of Computational Nanotechnology*, edited by M. Rieth and W. Schommers (American Scientific, Stevenson Ranch, CA, 2005).
- ³⁰J. Bass and W. P. Pratt Jr., *J. Phys. Condens. Matter* **19**, 183201 (2007).
- ³¹I. A. Campbell and A. Fert, *Ferromagnetic Materials* **3**, 797 (1982).
- ³²T. T. Chen and V. A. Marsocci, *Physica* **59**, 498 (1972).
- ³³T. R. McGuire and R. I. Potter, *IEEE Trans. Magn.* **11**, 1018 (1975).
- ³⁴É. M. Épshtein, *Phys. Solid State* **44**, 1327-1329 (2002).